Verification and Calculation of Negative Refractive Indices of a Meta-Material by Numerical Method *

SUI Qiang(隋强)[1,2], LIU Ci-Xiang(刘慈香)[1], LI Chao(李超)[1], LI Fang(李芳)[1**]

[1] *Institute of Electronics, Chinese Academy of Sciences, Beijing 100080*

[2] *School of Information, Communication University of China, Beijing 100024*

(Received 28 January 2005)

The verification and calculation of the negative refractive index of a meta-material is carried out by the finite-difference time-domain method. A slab and a prism of the meta-material are simulated. A genuine plane wave is generated by a two-direction periodic boundary condition (PBC) in the slab model. Based on an advanced phase extraction technique, the negative refractive index of the meta-material is verified by phase velocity measurement in the slab and prism measurement. From our results, not only the phenomenon of backward phase propagation but also the negative refraction is clearly observed. The index is also calculated precisely. The results from the two models are consistent.

PACS: 78. 20. Ci, 41. 20. Jb, 42. 70. Qs

In recent years, the study of meta-materials with negative permittivity and permeability has become a quite popular topic due to the realization of artificial arrangement of rods and split-ring resonators (SRRs). In 1968, Veselago[1] predicted that the electromagnetic wave propagation in a medium with simultaneous negative permittivity and permeability should give rise to several peculiar characteristics such as a negative refractive index, a reversed Doppler effect, and a reversed Cerenkov radiation. From 1996 to 1999, Pendry *et al.*[2−4] proposed an artificial system made of periodically interspaced conducting nonmagnetic split ring resonators (SRRs) and continuous metallic wires, which exhibits negative effective permeability and permittivity. Several experiments and simulations have been carried out to study the properties of meta-materials.[5−15] Moss *et al.*[16] studied the meta-material with the finite-difference time-domain (FDTD) method according to the experimental setup, in which the meta-material was restricted to two parallel PEC (Perfect Electrically Conducting) plates.

In this Letter, a more effective and accurate FDTD method is used to study the negative index of a meta-material. The two-direction periodic boundary condition (PBC)[17] is applied to generate the genuine plane wave, which makes the model of incident waves more precise. By extracting the phase from the simulated field pattern, the phase velocity and the direction of the wave front propagation can be obtained. Then, the refractive index of the meta-material is calculated by measuring the phase velocity in the slab model and by measuring the direction of wave front leaving the interface of the meta-material and air. The results from the two methods are consistent.

In this study, two models of the meta-material, i.e.

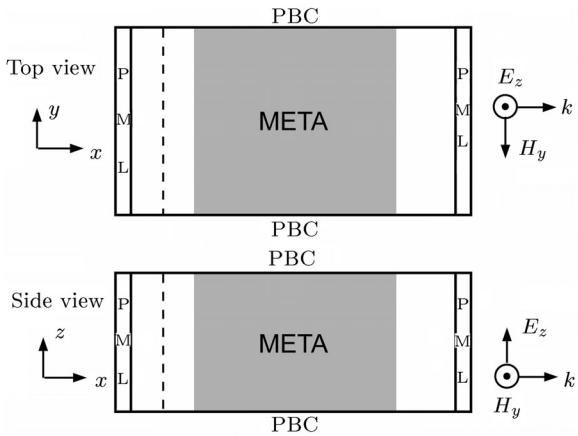


Fig. 1. The FDTD computational domain of the phase measurement.

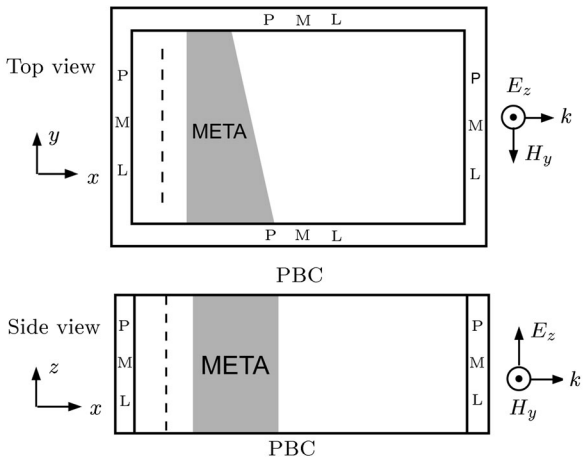


Fig. 2. The computational domain of the prism measurement.

* Supported by the National Basic Research Programme of China under Grant No 2004CB719800, and the National Natural Science Foundation of China under Grant No 60271027.

** To whom correspondence should be addressed. Email: fli@mail.ie.ac.cn

©2005 Chinese Physical Society and IOP Publishing Ltd

a slab and a prism, are simulated. The FDTD computational domain and their boundary condition are shown in Figs. 1 and 2.

In the model of a slab (Fig. 1), the PBC is applied in the y and z directions. That is, the slab is infinitely long in the two directions. Accordingly, the current sheet (indicated by the dashed line in Fig. 1) generates the genuine plane wave, which makes the model of incident waves more precise. This satisfies the conditions of Pendry's models.[2−4] In the x direction, perfectly matched layers (PMLs)[18] are applied to absorb the waves travelling outward. In the model of a prism (Fig. 2), the PBC is only applied in the z direction and the computational domain is surrounded by PMLs in the x and y directions.

The meta-material structure composed of periodic arrangement of rods and split ring resonators (SRRs) is chosen for study. The dimension of the meta-material unit is illustrated in Fig. 3. The discretization size is 0.25 mm and the time step is 3.85×10^{-4} ns. The structure contains $300\times20\times16$ cells in the slab model and $480\times420\times16$ cells in the prism model. The PMLs are in thickness of eight cells in both the models. Two types of the meta-material are studied in this work. For type 1, the structure is shown in Fig. 3 with the substrate $\varepsilon = 1.0$, which means that the space surrounding the metal structures is filled of air. For type 2, the structure is shown in Fig. 3 with the substrate $\varepsilon = 2.1$, which means that the 1-mm-thick Teflon is located between the rod and the SRR.

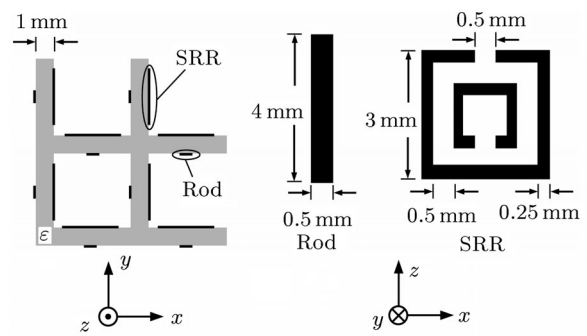


Fig. 3. Structure of the meta-material unit in our simulation.

The lattice constant is 5 mm. The SRRs and rods are modelled as the PEC material in the standard fashion by setting the tangential electric fields to zero.

In the FDTD simulation, if the incident wave is dependent on time in a sine form, the calculated field can reach a steady state in a later time step. Then the electric field in time t and position $\boldsymbol{r}$ can be expressed as $E_z(t,\boldsymbol{r}) = E_0(\boldsymbol{r})\cos[\phi_0(\boldsymbol{r}) - \omega t]$. The electric field at two different time t_1 and t_2 are expressed by

$$E_z(t_1,\boldsymbol{r}) = E_0(\boldsymbol{r})\cos[\omega t_1 - \phi_0(\boldsymbol{r})], \quad (1)$$

$$E_z(t_2,\boldsymbol{r}) = E_0(\boldsymbol{r})\cos[\omega t_2 - \phi_0(\boldsymbol{r})]. \quad (2)$$

Formula (2) can be written as

$$\begin{aligned} E_z(t_2,\boldsymbol{r}) &= E_0(\boldsymbol{r})\cos[\omega t_2 - \phi_0(\boldsymbol{r})] \\ &= E_0(\boldsymbol{r})\cos[\omega t_1 - \phi_0(\boldsymbol{r}) + \omega\Delta t] \\ &= E_z(t_1,\boldsymbol{r})\cos(\omega\Delta t) - E_0(\boldsymbol{r}) \\ &\quad \cdot \sin[\omega t_1 - \phi_0(\boldsymbol{r})]\sin(\omega\Delta t), \end{aligned} \quad (3)$$

where $\Delta t = t_2 - t_1$ (Δt is chosen approximately to be $T/4$ in the phase extraction). We can obtain

$$E_0(\boldsymbol{r})\sin[\omega t_1 - \phi_0(\boldsymbol{r})] = \frac{E_z(t_1,\boldsymbol{r})\cos(\omega\Delta t) - E_z(t_2,\boldsymbol{r})}{\sin(\omega\Delta t)}. \quad (4)$$

From Eqs. (1) and (4), the expression for phase reads

$$\begin{aligned} \phi(\boldsymbol{r},t_1) &= \omega t_1 - \phi_0(\boldsymbol{r}) \\ &= \arctan\left[\frac{E_z(t_1,\boldsymbol{r})\cos(\omega\Delta t) - E_z(t_2,\boldsymbol{r})}{\sin(\omega\Delta t)E_z(t_1,\boldsymbol{r})}\right]. \end{aligned} \quad (5)$$

At this point, the phase of E_z at arbitrary point $\boldsymbol{r}$ at time t_1 can be extracted by the simulated field pattern according to Eq. (5). Then, the phase velocity v_p and the direction of the wave front propagation can be obtained. The total time is divided into 40000 steps in our simulation.

The frequency band in which the meta-material exhibits simultaneously negative permittivity and permeability is determined by using a wideband pulse incident source, in the model as shown in Fig. 1. In our simulation, the first derivative of a Blackman–Harris[19] pulse is added as the source. The frequency band can be obtained by analysing the spectrum of the transmitted signal. Figure 4 shows the calculated results of normalized transmitted power in types 1 and 2. It is found that a narrow passband exists between 12.3 GHz and 12.8 GHz for type 1 and between 10.0 GHz and 10.5 GHz for type 2. In both the passbands, the backward wave property exists, which is verified in the phase measurement and in the prism measurement.

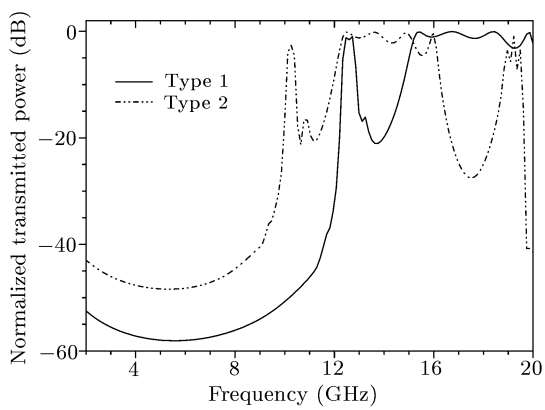


Fig. 4. Normalized transmitted power in types 1 and 2.

In the narrow passband, the electric field value through the centre of the type-1 meta-material at

12.468 GHz is shown in Fig. 5, and of the type-2 meta-material at 10.13 GHz is shown in Fig. 6. From Figs. 5 and 6, it is obvious that the phase velocity in the meta-material area is backward while forward in the air area. The field in the region of 20 mm<distance<57.5 mm contains both the incident field and the reflected field. Hence the slope in this region is nonlinear while it is linear in the region of distance>132.5 mm and distance<20 mm. The wave front movement inside the meta-material is illustrated clearly, which can not be observed in experiment.

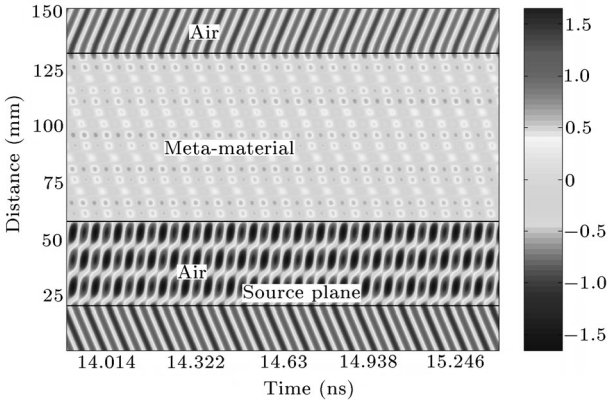


Fig. 5. Electric field value through the type-1 meta-material at 12.468 GHz.

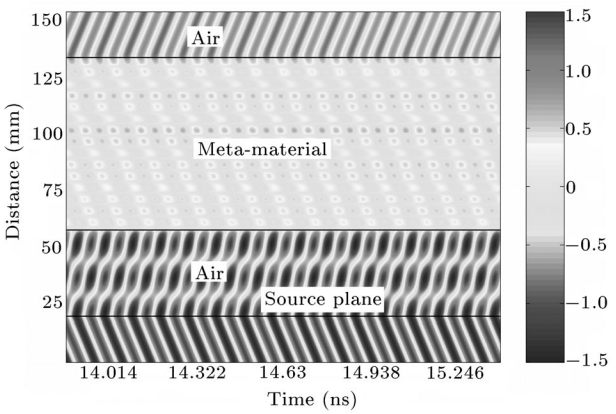


Fig. 6. Electric field value through the type-2 meta-material at 10.13 GHz.

Another effective method to verify the property of meta-material is to measure the direction of the wave front leaving the interface of the prism. For comparison, a prism of homogeneous dielectric Teflon ($\varepsilon_r = 2.1$) is simulated. A staircased approximation of the $\alpha = 18.4°$ interface is used to model the Teflon prism. Figure 7 shows the electric field pattern in the calculation domain.

In order to build a meta-material prism, we again use a coarse staircasing approximation with the meta-material unit cells (Fig. 3). To build the $\alpha = 18.4°$ interface, we use three SRRs in the y axis for every single SRR in the x axis. The electric fields are shown in Figs. 8 and 9 for the prism made of types 1 and 2, respectively. From Figs. 7–9, it is found that the refractive wave leaving the interface between the air and Teflon is bent towards the other side of the normal, while the one leaving the interface between the meta-material and the air is bent towards the same side of the normal.

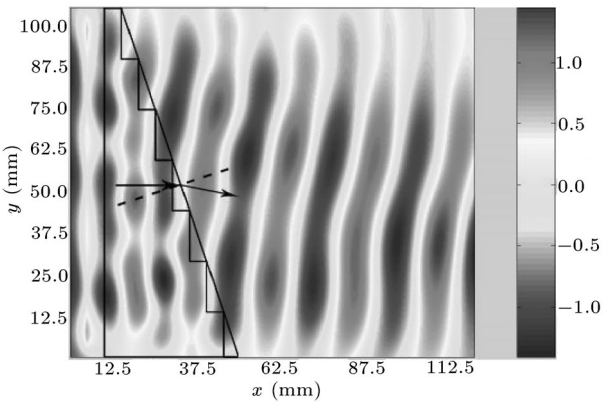


Fig. 7. Electric field value through the prism of Teflon.

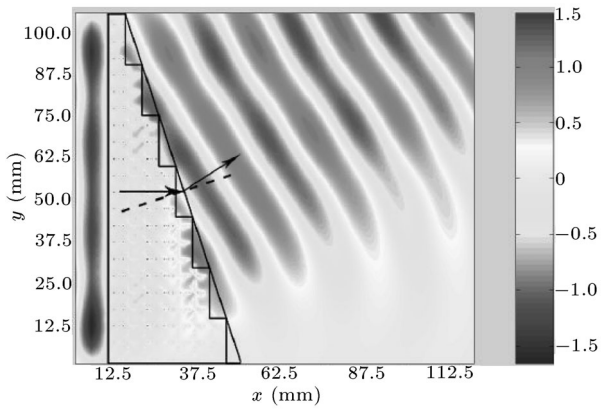


Fig. 8. Electric field value through the type-1 prism at 12.468 GHz.

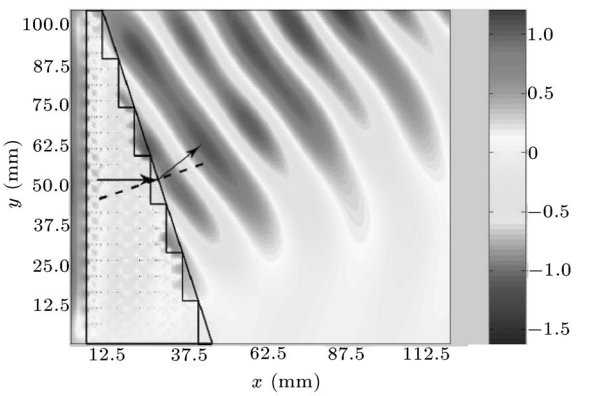


Fig. 9. Electric field value through the type-2 prism at 10.13 GHz.

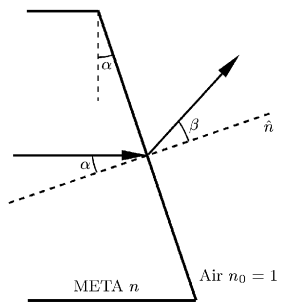


Fig. 10. Snell's law in the prism measurement.

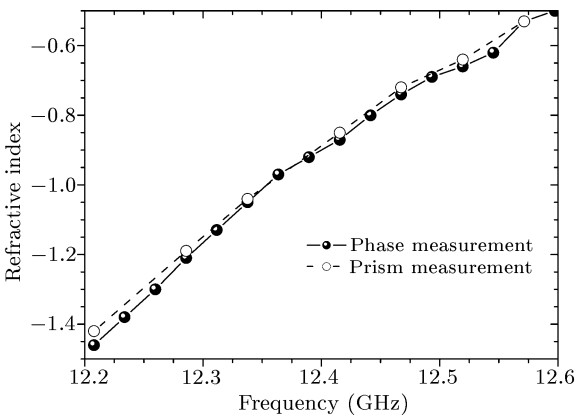


Fig. 11. Calculated index as a function of frequency of type 1.

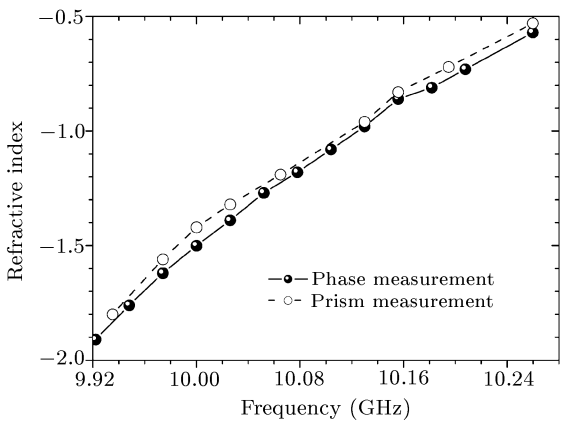


Fig. 12. Calculated index as a function of frequency of type 2.

The refractive index can be obtained by $n = c/v_p$ or by the refraction angle. Using Snell's law we have $n = p\left|\frac{\sin\beta}{\sin\alpha}\right|$ (as shown in Fig. 10), where α is the angle between the incident ray and the normal, β is the angle between the refracted ray and the normal. If the incident ray and the refracted ray are on the same side of the normal, we can obtain $p = -1$; otherwise $p = 1$. By using different frequency sine wave sources, the refractive index versus the frequency is calculated by the phase measurement and the prism measurement. The results are illustrated in Fig. 11 for type 1 and Fig. 12 for type 2.

In summary, phase measurement and prism measurement based on the FDTD method have been applied to determine the negative refractive index. The genuine plane wave is generated by a two-dimensional PBC to make the model of incident waves more precise than previous experimental setups. The backward phase movement in the meta-material is observed clearly. The refractive wave leaving the interface between the air and the meta-material is bent on the same side of the normal. The refractive index can be calculated with Snell's law in the prism measurement and with phase extraction in a slab of the meta-material. The results from the two methods are consistent. The two-dimensional PBC and phase extraction technique, which cannot be realized in experiment, are effective tools to study the composite meta-materials composed of rods and SRRs.

References

[1] Veselago V G 1968 *Sov. Phys. Usp.* **10** 509
[2] Pendry J B, Holden A J, Stewart W J et al 1996 *Phys. Rev. Lett.* **76** 4773
[3] Pendry J B, Holden A J, Robbins D J et al 1998 *J. Phys.: Condens. Matter.* **10** 4785
[4] Pendry J B, Holden A J, Robbins D J et al 1999 *IEEE Trans. Microwave Theor. Technol.* **47** 2075
[5] Smith D R, Padilla W J, Vier D C et al 2000 *Phys. Rev. Lett.* **84** 4184
[6] Shelby R A, Smith D R and Schultz S 2001 *Science.* **292** 77
[7] Quan B, Chao L, Sui Q et al 2005 *Chin. Phys. Lett.* **22** 1243
[8] Stefan E, Gerard T, Pierre S et al 2002 *Phys. Rev. Lett.* **89** 213902-1
[9] Zhang F L, Zhao Q, Liu Y H et al 2004 *Chin. Phys. Lett.* **21** 1330
[10] Chen H S, Ran L X, Huangfu J T et al 2003 *J. Appl. Phys.* **94** 3712
[11] Sui Q, Li C, Li L L et al 2004 *Prog. Electromagnet. Res.* **51** 281
[12] Bayindir M, Aydin K, Ozbay E et al 2002 *Appl. Phys. Lett.* **81** 120
[13] Ran L X, Zhang X M, Cheng K S et al 2003 *Chin. Sci. Bull.* **48** 1325
[14] Wang Y Q, Feng Z F, Hu X Y et al 2004 *Chin. Phys. Lett.* **21** 324
[15] Correia D and Jin J M 2004 *Microwave Opt. Tech. Lett.* **40** 201
[16] Moss C D, Grzegorczyk T M, Zhang Y et al 2002 *Prog. Electromagnet. Res.* **35** 315
[17] Allen T 2000 *A Computational Electrodynamics: The Finite-Difference Time-Domain Method* 2nd edn (Boston, MA: Artech House)
[18] Berenger J P 1994 *J. Comput. Phys.* **114** 185
[19] Harris F J 1978 *Proc. IEEE* **66** 51